

Scalable engineering of multipartite W states in a spin chain

Vinitha Balachandran¹ and Jiangbin Gong^{1,2}

¹*Department of Physics and Center for Computational Science and Engineering, National University of Singapore, Singapore 117542*

²*NUS Graduate School for Integrative Sciences and Engineering, Singapore 117597*

(Received 11 April 2012; published 4 June 2012)

We propose a scalable scheme for engineering multipartite entangled W states in a Heisenberg spin chain. The rather simple scheme is mainly built on the accumulative angular squeezing technique first proposed in the context of quantum kicked rotor for focusing a rotor to a delta-like angular distribution [I. Sh. Averbukh and R. Arvieu, *Phys. Rev. Lett.* **87**, 163601 (2001)]. We show how the efficient generation of various W states may be achieved by engineering the interaction between a spin chain (short or long) and a time-dependent parabolic magnetic field. Our results may further motivate the use of spin chains as a test bed to investigate complex properties of multipartite entangled states. We further numerically demonstrate that our scheme can be extended to engineer arbitrary spin chain quasimomentum states as well as their superposition states.

DOI: [10.1103/PhysRevA.85.062303](https://doi.org/10.1103/PhysRevA.85.062303)

PACS number(s): 03.67.Bg, 05.45.Mt, 75.10.Pq

I. INTRODUCTION

Entanglement is a unique quantum property featuring nonlocal correlations between two or more quantum systems [1]. Over the past few decades there has been an increasing interest in studies of entanglement [2]. The main motivations are the potential advantages offered by entanglement in quantum information tasks such as quantum teleportation [3], quantum cryptography [4], and quantum computation [5]. So far early studies focused mainly on entanglement between two systems termed as bipartite entanglement. The preparation, characterization, and quantification of bipartite entanglement are now fairly well understood. By contrast, the case of multipartite entanglement (i.e., the entanglement between three or more particles) is still much less understood. Attempts to extend the ideas of bipartite entanglement to many-body systems have led to the finding of different classes of multipartite entangled states [6].

A particularly important multipartite state that has attracted much attention is the so-called W state. An N -qubit W state consists of a superposition of N states where exactly one qubit is in state $|1\rangle$ while all the others are in state $|0\rangle$ [6]. A W state can be represented as

$$|W_N\rangle = \frac{1}{\sqrt{N}}(|100\cdots 0\rangle + |010\cdots 0\rangle + \cdots |000\cdots 1\rangle). \quad (1)$$

Entanglement of a W state is robust against the qubit loss (i.e., if some qubits are lost the remaining qubits are still entangled [7]). Also, the entanglement is immune against global dephasing and qubit flip noise [8]. Owing to these interesting properties, W states play a more important role than other entangled multipartite states for practical applications in quantum information processing [9]. Hence, the efficient generation of W states is of particular interest.

Numerous schemes have been proposed and demonstrated for engineering W states using photons as qubits [10]. Although photons are advantageous for distant communication, the resources required to entangle photons grows exponentially with the increase in photon number. Alternatively, the preparation of W states in cavity quantum electrodynamics (QED) systems and ion traps have been discussed [11]. Nevertheless, the problem of scalability still remains unresolved. Recently,

a robust scheme generating W states in cavity QED systems with improved scalability was introduced [12]. However, that linear-optics-based scheme requires post selections. Another system investigated for the generation of W states is spin chains. In contrast to the above-mentioned systems, spin chains may require less resources. For instance, the natural evolution of XY spin chains was shown to generate three or four qubit W states at specific times [13]. The need for instantaneous measurement at specific times and the lack of generalization to systems with more qubits are the main disadvantages of such a method based on the natural evolution of spin chains. Other approaches used branched spin chains [14] or used engineered defects in an anisotropic spin chain [15] to generate W states. These approaches require individual addressing of spins and hence are not straightforward to implement.

In this paper, we examine a simple and *scalable* scheme for efficient controlled generation of N -qubit W states in a Heisenberg spin chain using instantaneous pulses of an external parabolic field. The central idea of such a scheme, based on an intriguing mapping between the dynamics of a kicked spin chain with that of a quantum kicked rotor [16], is essentially the angular squeezing technique previously studied in the context of quantum rotor dynamics [17]. Our scheme has a few obvious advantages. First, it requires only control over the global parameters of the spin chain, such as the strength of the parabolic magnetic field and the timing of applied control pulses. Second, it does not require any measurement at any particular times: a W state is guaranteed to emerge at the end of a controlled evolution process. Third, single spin chain quasimomentum states and their superposition states can be engineered in an analogous manner, thus resulting in the generation of a whole class of generalized W states. But most important of all, our scheme is scalable in the sense that it equally applies no matter how long the spin chain becomes. That is, in principle, the engineering scenario itself is largely independent of the number of qubits.

This paper is organized as follows. In Sec. II, we introduce the spin chain model used in our study. This is followed by introducing a mapping between a kicked spin chain and a quantum kicked rotor. We then briefly introduce in Sec. II C the technique proposed earlier for focusing quantum rotors to

δ -like angular distributions. In Sec. III, we present our scheme for the generation of W states in spin chains and numerically investigate its performance and its extensions. Finally, we conclude the paper in Sec. IV.

II. GENERAL CONSIDERATIONS

A. Heisenberg spin chain

Let us start from a Heisenberg chain of N spins with the Hamiltonian

$$H_{\text{hc}} = -J \sum_{n=1}^{N-1} \sigma_n \cdot \sigma_{n+1}. \quad (2)$$

Here $\sigma \equiv (\sigma^x, \sigma^y, \sigma^z)$ are the Pauli matrices and J is the coupling strength between nearest-neighbor spins. Also, we assume that all system parameters have been appropriately scaled and take dimensionless values, with $J = 1$, $\hbar = 1$ throughout. The dynamics of the above spin chain conserves the total polarization $S_z \equiv \sum_{n=1}^N \sigma_n^z$. To simplify the matter we focus on the single excitation subspace (that is, states with $N - 1$ spins up and one spin down, denoted by $|\mathbf{m}\rangle = \sigma_m^+ |000 \cdots 0\rangle$, with $m = 1, 2, \dots, N$). For periodic boundary conditions (open-ended chains will be discussed later), the eigenvectors for the single spin-flip sector of the Hamiltonian in Eq. (2) (in terms of the basis states $|\mathbf{m}\rangle$) are

$$|k\rangle = \frac{1}{\sqrt{N}} \sum_{m=1}^N e^{imk} |\mathbf{m}\rangle. \quad (3)$$

These states represent spin waves or magnons with quasimomentum $k = (-N + 2n)\pi/N$ where $n = 1, 2, \dots, N$. For this reason we call states $|k\rangle$ as quasimomentum states below. The energy eigenvalues of these states are given by (up to a constant)

$$E_k = -J \cos(k). \quad (4)$$

From Eq. (3), it follows that all the eigenstates can be regarded as generalized W states with certain phases between the different single spin-flip states. In particular, the $|k=0\rangle$ state is the symmetric W state given in Eq. (1).

B. Quantum kicked rotor model and the Heisenberg spin chain model

Applying an external parabolic δ -pulsed magnetic field to the Heisenberg spin chain, the Hamiltonian reads

$$H = H_{\text{hc}} + \frac{C}{2} \sum_{n=1}^N (n - n_0)^2 \sigma_n^z \sum_j \delta(t - jT_0). \quad (5)$$

Here C and n_0 are the amplitude and the central position of the parabolic field and T_0 is the kicking period. Note that the δ pulses still conserve the total polarization and therefore the dynamics is still restricted to the single excitation subspace. As the Hamiltonian H is periodic in T_0 , we have $|\psi(t = (j + 1)T_0)\rangle = U(T_0)|\psi(t = jT_0)\rangle$, where $U(T_0)$ is given by

$$U(T_0) = U^{\text{kick}} U^{\text{free}} = e^{(-iC/2) \sum_{n=1}^N (n - n_0)^2 \sigma_n^z} e^{-iT_0 H_{\text{hc}}}. \quad (6)$$

Here $U^{\text{kick}} = e^{(-iC/2) \sum_{n=1}^N (n - n_0)^2 \sigma_n^z}$ and $U^{\text{free}} = e^{-iT_0 H_{\text{hc}}}$, with

$$\langle \mathbf{m} | U^{\text{kick}} | \mathbf{n} \rangle = e^{(-iC/2)(n - n_0)^2} \delta_{mn}. \quad (7)$$

Further, in the limit of large N , we have

$$\langle \mathbf{m} | U^{\text{free}} | \mathbf{n} \rangle \approx i^{m-n} J_{m-n}(JT_0), \quad (8)$$

where J_n represents the Bessel function of order n [16]. It is interesting to note that the above matrix elements of $U(T_0)$ are very similar to the matrix elements of the evolution operator of a quantum kicked rotor (QKR) [16], the standard model used in the quantum chaos literature, whose Hamiltonian is given by

$$H_{\text{QKR}} = \frac{(\hat{p} - p_0)^2}{2} - K \cos(\hat{\theta}) \sum_j \delta(t - jT), \quad (9)$$

where K is the strength and T is the period of the kick. Indeed, the matrix elements of the time evolution operator of QKR (in terms of its momentum basis states $|m\rangle = e^{im\theta}/\sqrt{2\pi}$ for an effective Planck constant \hbar) are given by the product of two terms

$$\begin{aligned} \langle m | U_{\text{QKR}}^{\text{free}} | n \rangle &= e^{-i\hbar(n - n_0)^2/2} \delta_{mn}, \\ \langle m | U_{\text{QKR}}^{\text{kick}} | n \rangle &= i^{m-n} J_{m-n} \left(\frac{K}{\hbar} \right), \end{aligned} \quad (10)$$

with period $T = 1$. The first line in Eq. (10) corresponds to the free evolution whereas the second line depicts the effect of the kicking potential. Comparing Eqs. (7) and (8) with Eq. (10), it is clear that the free evolution part of the Heisenberg spin chain is parallel to the kicking part of the QKR evolution operator, whereas the U^{kick} operator associated with the parabolic magnetic field in the spin chain case is parallel to $U_{\text{QKR}}^{\text{free}}$. Indeed, this mapping becomes clearer if we rewrite Eq. (2) in terms of the quasimomentum states $|k\rangle$ as

$$H_{\text{hc}} = -J \sum_k \cos(k) |k\rangle \langle k|. \quad (11)$$

Thus, the quasimomentum (k) of the spin chain maps onto the angular position operator ($\hat{\theta}$) in the QKR. Similarly, the site index (n) can be mapped onto the momentum (\hat{p}/\hbar) in the QKR. Further, we can identify the mappings $JT_0 \rightarrow \frac{K}{\hbar}$, $C \rightarrow \hbar$ and $|\mathbf{m}\rangle \rightarrow |m\rangle$.

With the aid of this mapping, one can now use tools from the control of QKR dynamics to control the dynamics of spin chains. For instance, using this mapping the controlled transfer of quantum information and the controlled amplification of spin excitation have been proposed by us [18]. For our study here, because a W state corresponds to a state with zero quasimomentum (i.e., $|k=0\rangle$), the issue of the efficient generation of the W state in the spin chain is equivalent to the alignment or focusing of rotors to the zero angular position state $|\theta=0\rangle$. Fortunately, the authors of Ref. [17] already proposed how to focus a quantum rotor to the $|\theta=0\rangle$ state, as introduced in the next section.

C. Accumulative angular squeezing for focusing a quantum rotor

The degree of orientation or squeezing of a quantum rotor at $\theta = 0$ can be quantified by $D_{\text{QKR}} = \langle 1 - \cos(\hat{\theta}) \rangle$. If the rotor

is entirely in the $|\theta = 0\rangle$ state, then D_{QKR} has its minimum value of 0. To efficiently and successively decrease the value of D_{QKR} , Averbukh and Arvieu proposed a simple solution by manipulating the time intervals between two neighboring kicks [17]. The strategy goes as follows. After the first kick at time $t_1 = 0$, the maximal squeezing occurs after a time delay Δt_1 . Now let a second kick be applied at time $t_2 = \Delta t_1$. Immediately after the second kick, the probability density distribution of θ remains the same. However, the degree of squeezing then evolves in time before a third kick comes in. During the free evolution, $D_{\text{QKR}}(t)$ and its derivative are continuous and periodic functions of time. Thus, $D_{\text{QKR}}(t)$ will reach a new minimum at a new time $t_2 + \Delta t_2$ in the interval $[t_2, t_2 + 4\pi]$ (Note that the dynamics of a free quantum rotor is fully periodic with a period of 4π). The new minimal value of the degree of squeezing should be less than that of the previous one. By continuing this (i.e., applying kicks at time $t_{j+1} = t_j + \Delta t_j$) with the following time evolution operator

$$\begin{aligned} \dots e^{-i\Delta t_3 \frac{(\hat{p}-p_0)^2}{2\hbar}} e^{-i\frac{K}{\hbar} \cos \hat{\theta}} e^{-i\Delta t_2 \frac{(\hat{p}-p_0)^2}{2\hbar}} \\ \times e^{-i\frac{K}{\hbar} \cos \hat{\theta}} e^{-i\Delta t_1 \frac{(\hat{p}-p_0)^2}{2\hbar}} e^{-i\frac{K}{\hbar} \cos \hat{\theta}}, \end{aligned} \quad (12)$$

the squeezing effects accumulate in time. It has been numerically shown that the logarithm of D_{QKR} decreases successively without any sign of saturation. Theoretical considerations [17] further suggested that for a large number of kicks, the angular variance at the j th kick, denoted $\langle \hat{\theta}^2 \rangle_j$, is inversely proportional to the square root of the kick number j and the required time delay Δt_j for the application of the j th kick is inversely proportional to the kick number (i.e., $\langle \hat{\theta}^2 \rangle_j \propto 1/\sqrt{j}$ and $\Delta t_j \propto 1/j$). Thus, unlimited squeezing in the region of $\theta = 0$ can be obtained for a quantum rotor. This strategy has been experimentally demonstrated using cold cesium atoms in a pulsed optical lattice [19]. For a given fixed number of kicks, further improvement over the accumulative squeezing can be obtained using optimal squeezing strategies, where the D_{QKR} value can be minimized in a high-dimensional space of all possible delay times $\Delta t_j > 0$ [20].

III. EFFICIENT GENERATION OF W STATES IN A SPIN CHAIN

A. Squeezing of quasimomentum distribution via a single kick

We are now ready to exploit the mapping between QKR and a kicked spin chain as well as the angular squeezing technique to investigate how W states can be generated with high fidelity and with high efficiency. To ensure that the mapping between QKR and a kicked spin chain is fairly accurate, we first consider a long chain of 200 spins. As mentioned previously, the similarity between the propagator of a QKR and a sufficiently long spin chain implies the following mapping:

$$\begin{aligned} e^{-it \frac{(\hat{p}-p_0)^2}{2\hbar}} &\rightarrow e^{-iC \frac{(n-n_0)^2}{2}}, \\ e^{-i\frac{K}{\hbar} \cos(\hat{\theta})} &\rightarrow e^{-itJ \cos(k)}, \end{aligned} \quad (13)$$

where t here is understood as the (yet-to-be-determined) free evolution time for a quantum rotor or a spin chain (in

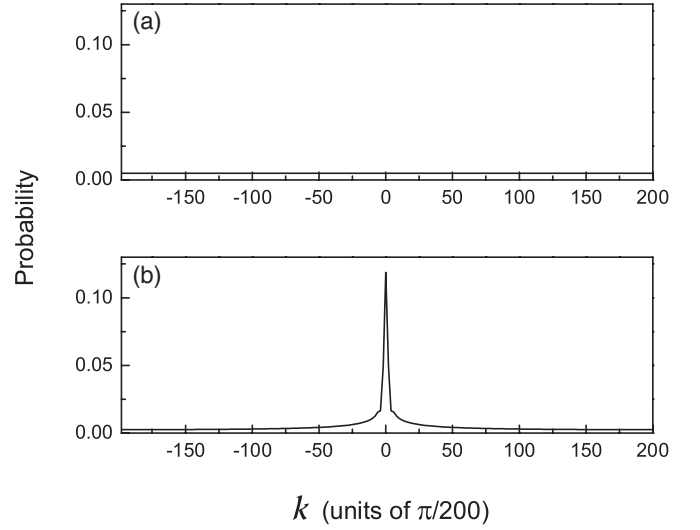


FIG. 1. (a) Quasimomentum distribution profile of a Heisenberg chain of 200 spins at time $t = 0$ and (b) after applying a kick of strength $C = 1/85$ at $t = 85$. The distribution after the kick is peaked at $k = 0$, indicating the formation of a W state. As mentioned in the main text, all plotted quantities here and in other figures take dimensionless values.

periodically driven cases, the fixed free evolution time is denoted by T or T_0). From Eq. (13) it is clear that a strong kick in the QKR implies long-time free evolution of a spin chain if we set $J = 1$. Also, the free evolution of duration t in the QKR with $\hbar = 1$ corresponds to kicking the chain with a field of appropriate strength C . For example, for quantum rotor squeezing using one strong kick only, a semiclassical consideration for QKR suggests that a strong kick with strength K will yield squeezing at time $t = 1/K$ [17]. Its spin chain analog then becomes the following (after doing the mapping): we first evolve the chain for long time t and then kick the chain with a parabolic field with strength $C = 1/t$. Figure 1 demonstrates that this understanding is correct at the single kick level. There, the initial state is a single spin excitation at the center of the chain (i.e., $\Psi_{\text{in}} = |\mathbf{100}\rangle$). From Eq. (3), it follows that all the quasimomentum states have equal probability (i.e., $|c_k|^2 = 1/200$ where c_k is the probability amplitude of a state with quasimomentum k) as shown in the top panel of Fig. 1. The chain is then evolved until time $t = 85$, after which a kick of strength $C = 1/85$ is applied. The bottom panel of Fig. 1 shows the probability distribution in the quasimomentum space of the quantum state right after applying the kick. It is clear that focusing at the $|k = 0\rangle$ state occurs at this field strength. To characterize the squeezing in the k space, we use $D = \langle 1 - \cos(k) \rangle$ for the spin chain case. It is interesting to note that we obtained the same value of $D = 0.418$ as obtained for QKR as the authors of Ref. [17], constituting a direct proof that the angular squeezing technique for QKR can be translated to the spin chain context. This is the case, even though in our calculations the spin chain has a finite number of spins. Note also that we have carried out similar calculations for open-ended spin chains (that is, without using the periodic boundary condition) and similar results were obtained.

B. Accumulative squeezing for the generation of W states

With the remarkable correspondence between the squeezing dynamics of a finite spin chain and that of a quantum rotor confirmed, it is interesting to investigate the usefulness of the above-mentioned accumulative angular squeezing strategy in enhancing the focusing on the $k = 0$ quasimomentum state of the spin chain (hence leading to the efficient generation of a W state). Because the kicking part in the QKR case corresponds to the free evolution part in the spin chain, in our scheme we first evolve the chain for a fixed duration t . From the mapping between the QKR free evolution and the kicking part of the spin chain, the second step in our scheme is to kick the spin chain with a particular field C_j that minimizes the function $\langle 1 - \cos(k) \rangle$. These two steps constitute one loop. By iterating the loops (i.e., by considering the following total time evolution operator)

$$\dots e^{-iC_3 \frac{(n-n_0)^2}{2}} e^{-itH_{hc}} e^{-iC_2 \frac{(n-n_0)^2}{2}} \times e^{-itH_{hc}} e^{-iC_1 \frac{(n-n_0)^2}{2}} e^{-itH_{hc}}, \quad (14)$$

the expectation value $\langle 1 - \cos(k) \rangle$ that characterizes the degree of squeezing D can be minimized and hence one obtains a state sharply localized at $k = 0$, which is just a W state of the chain. Figure 2 presents one computational example of the accumulative focusing to the $|k = 0\rangle$ state in a chain of 200 spins, with the free evolution time t fixed at $t = 3.0$ (i.e., with period $T_0 = 3.0$). In particular, the top panel of Fig. 2 depicts the degree of squeezing D after each kick and bottom panel shows the optimized field strength C associated with each kick. Here we used the same initial state $\Psi_{in} = |\mathbf{100}\rangle$ used in Fig. 1, whose initial value of D is unity. The chain is

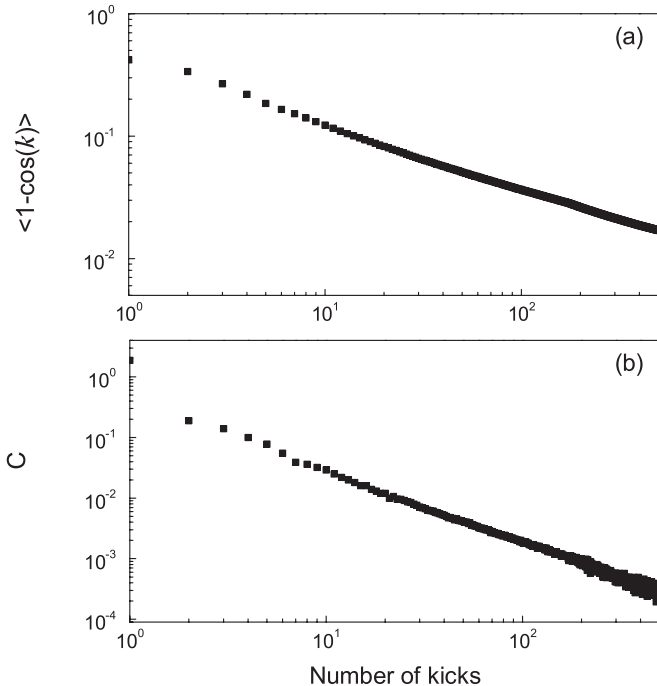


FIG. 2. Accumulative squeezing onto a W state for a Heisenberg chain of 200 spins. Panel (a) shows the variation of degree of squeezing $D = \langle 1 - \cos(k) \rangle$ with the number of kicks whereas panel (b) shows the field strength C used for each kick.

first evolved for a duration of $t = 3.0$ and we then apply the first kick of strength $C = 1.87$. Right after the first kick D becomes 0.42. Upon a second kick of strength $C = 0.19$, D is further reduced to 0.33. Note that the particular values of field strength are those that minimize D for each kick. This process then continues.

It is also necessary to elaborate on how the minimization of D is done at each loop of iteration. In particular, the minimal value of D is searched by scanning the value of C in a certain range $[C_l, C_h]$, where the choices of C_l and C_h can be made by making an analogy to the squeezing dynamics of QKR. For QKR, the expectation value D_{QKR} initially decreases with a decreasing pulse interval Δt_1 and then increases. The chosen value of $t_2 = \Delta t_1$ for the second kick in the QKR case is when D_{QKR} reaches the minimal value before its increase. After the kicking at time t_2 , D_{QKR} again decreases with a decreasing pulse interval Δt_2 until $t_3 = \Delta t_2 + t_2$ where $t_2 < t_3$. In Ref. [17], $t_2 = 1.87$. In our spin chain calculations, we obtained the first optimal value of field strength by scanning C in the range $[0.1, 10]$. It is found that, similar to the QKR case, the value D decreases with C and then increases. Indeed the optimal value of C is also found to be 1.87. We then attempt to find the second optimized value of C by searching the minimal values of D for all values of C in the range $[C_l, 1.87]$. This process then continues. That is, C_h is the optimal value of C for the previous kick and C_l is a value set to be much less than C_h . Note that the value of C_l is adjusted for each kick to ensure that the increase in D with decreasing C can be encountered.

It is clear from Fig. 2(a) that the value of $D = \langle 1 - \cos(k) \rangle$ successively decreases with more kicks. We even found that the D values assume almost the same values of D_{QKR} as mentioned in Ref. [17]. Also, for a large number of kicks, we find that the D value is inversely proportional to \sqrt{M} , where M is the number of kicks, and the optimized field strength C is inversely proportional to M , both aspects being parallel to the case of QKR squeezing. All these observations indicate that so long as the spin chain is long enough (such that the spin chain dynamics is close to the QKR dynamics), then the scheme here to generate N -partite W states is *irrespective* of the actual number (N) of spins in the chain.

It must be noted, however, that the correspondence between QKR and a kicked Heisenberg spin chain is exact only in the limit of large N . Indeed, in a quantum rotor system, the momentum quantum number ranges from $-\infty$ to ∞ whereas in the spin chain here, the site index n is restricted to a finite range for a finite spin chain. So it is expected that some differences between QKR and a kicked spin chain will be pronounced for short spin chains. It is hence necessary to look into the feasibility of accumulative squeezing for relatively short spin chains. Our calculations show that D saturates after some finite number of kicks in cases of short chains. Once saturation arises, no further squeezing is possible using any field strength. For instance, for a chain of 20 spins, D saturates after 30 kicks. The number of kicks after which the saturation of D takes place decreases as the chain length decreases. Fortunately, we found that unlimited squeezing is still possible for short chains with a slight modification of the accumulative angular squeezing technique. This is the topic of next section.

C. W state generation in a short spin chain

Here we present a modified strategy to obtain unlimited squeezing to the $|k = 0\rangle$ state (or the W state) of a short spin chain. The scheme consists of iterations of the following two steps:

- (1) Evolve the chain freely until time t_j ;
- (2) At time t_j , apply a kick of strength C_j ,

where t_j and C_j are the optimized values of free evolution time and field strength, obtained by minimizing the D value right after the j th kick. Thus, iterating the control loops

$$\dots e^{-iC_3 \frac{(n-n_0)^2}{2}} e^{-it_3 H_{hc}} e^{-iC_2 \frac{(n-n_0)^2}{2}} \times e^{-it_2 H_{hc}} e^{-iC_1 \frac{(n-n_0)^2}{2}} e^{-it_1 H_{hc}}, \quad (15)$$

D can be successively minimized. The difference from what we did in the previous section is that here a two-dimensional optimization is performed for each control loop. Let us now turn to our numerical results based on this scheme. In Fig. 3, we show one particular example of our numerical findings for a chain of 20 spins only. We start with an initial state exclusively localized at the center of the chain (i.e., $|10\rangle$). This state corresponds to a completely delocalized state in the quasimomentum space of the spin chain. Hence the initial value of D is unity. For each control loop, we implement the two-dimensional minimization of D using the combined stimulated annealing and downhill simplex method of Nelder and Mead [21]. We further limit the values of C_j and t_j in the reasonable ranges $[0.001, 10]$ and $[0.001, 100]$, respectively. For the first kick, the minimal value of D is obtained when a field of strength $C_1 = 0.1495$ is applied at time $t_1 = 10.559$. As shown in Fig. 3, for this kick the D value reduces to 0.6351. For minimizing D further, we again numerically find optimized field strength $C_2 = 0.1886$ applied at time $t_2 = 30.5459$. The minimal value of D after the second kick is 0.4846. By applying a series of such optimized kicks, it is seen that D decreases without a sign of saturation, even though the

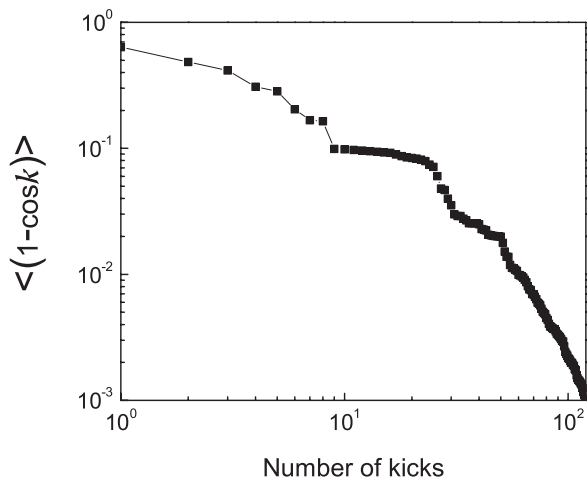


FIG. 3. Variation of $\langle 1 - \cos(k) \rangle$ with the number of kicks for a chain of 20 spins. Here the strength of the pulses C is varied between $[0.001, 10]$. Also, the free evolution time t of the chain between two neighboring kicks is varied between $[0.001, 100]$. The expectation value $\langle 1 - \cos(k) \rangle$ decreases successively with the number of control pulses. Note that for the W state $\langle 1 - \cos(k) \rangle = 0$.

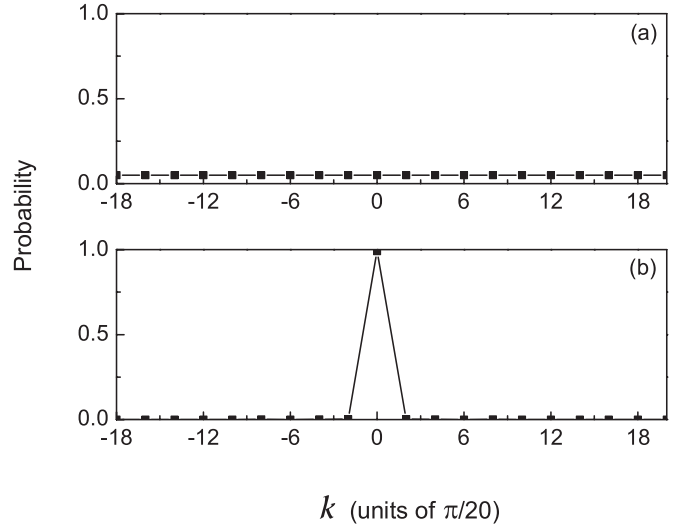


FIG. 4. Probability distribution in the quasimomentum space of a chain of 20 spins. Panel (a) represents the initial distribution and panel (b) represents the distribution after applying 80 pulses. Here the strength of the pulses C is varied in the range $[0.001, 10]$ and the free evolution time t of the chain between two neighboring kicks is varied between $[0.001, 100]$.

chain only has 20 spins. We also note that by increasing the range for C_j and t_j in the two-dimensional optimization, even lower values of D can be obtained for a fixed number of kicks, though the improvement might not be that significant. For instance, after 50 kicks the D value for the above-mentioned ranges of C_j and t_j is 0.01989. An increase in the range of C_j and t_j to $[10^{-8}, 10]$ and $[10^{-8}, 100]$ can further slightly decrease D to 0.00557.

Figure 4 illustrates the high fidelity of our scheme in generating the W state. There the quasimomentum distribution profile of the chain with 20 spins is plotted after 80 optimized kicks. As seen from Fig. 4(b), more than 99% population is transferred to the $|k = 0\rangle$ state. For the shown final state, the D value that characterizes the fidelity of the W state is as low as 4.51×10^{-3} .

Next, we compare the state generated by our scheme with the perfect W state. To that end we use the global entanglement measure E_{global} as introduced by Meyer and Wallach [22] (here global entanglement is used as one convenient measure, not meant to be the most strict measure for genuine N -partite entanglement). E_{global} is related to the averaged one-qubit purity

$$E_{\text{global}} = 2 \left(1 - \frac{1}{N} \sum_{i=1}^N \text{Tr}[\hat{\rho}_i^2] \right), \quad (16)$$

where $\hat{\rho}_i$ is the density matrix of the i th spin after tracing over all other spins in the system. As shown in Ref. [22], E_{global} for a W state of chain of N spins is $4(N-1)/N^2$. Hence for $N = 20$, $E_{\text{global}} = 0.19$. We find that for the state plotted in Fig. 4, $E_{\text{global}} = 0.1899$. Note also that the $|k = 0\rangle$ state is a stationary eigenstate of our bare spin chain with Hamiltonian H_{hc} under the periodic boundary condition. Hence the generated state $|k = 0\rangle$ does not evolve with time even after the removal of the pulsed parabolic magnetic field. To further characterize

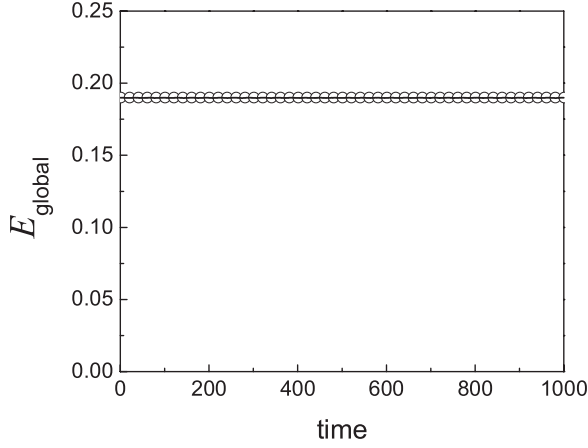


FIG. 5. Time evolution of the global entanglement E_{global} under the Hamiltonian given in Eq. (2) with $N = 20$ (circles). Initially, the chain is assumed to be in the engineered state given in Fig. 4(b). Straight line denotes the theoretical value of E_{global} for the W state.

the fidelity of our generated W state, we have investigated the dynamics of global entanglement in the chain after we switch off the parabolic field. Because the final product state is not exactly the $|k = 0\rangle$ state, the value of E_{global} varies slightly with time. However, this variation is vanishingly small. In particular, for a chain of 20 sites the value of E_{global} for our engineered final state in Fig. 4(b) varies between 0.1897 and 0.19. This is illustrated in Fig. 5. The straight line there corresponds to the theoretical value of global entanglement for a perfect W state. It is seen that E_{global} remains extremely close to the theoretical value of 0.19.

In addition to the high fidelity in the generation of W states, our scheme offers several other advantages as compared to the existing ones. For instance, W states are generated by the controlled dynamics of the chain and hence do not require any instantaneous measurement at specific times to selectively measure the state. Another advantage is that we require only optimization over global parameters, such as the strength of the parabolic field and the timing of the control pulses.

To check the general applicability of our scheme, we have further investigated open-ended chains. Unlike the case of long chains, the dynamics of short chains are considerably different with open and periodic boundary conditions. However, our results show that our scheme also works with short open-ended chains, but with reduced fidelity. Compared to periodic chains, a larger number of kicks is required to obtain a low D value. For instance, the D value drops below 0.05 after 217 kicks in an open-ended chain of 20 spins whereas only 27 kicks are needed in a chain with periodic boundary conditions to reach similar degree of squeezing.

D. Generation of other states

Is it possible to generate other states by extending our scheme? We address this question in this section. First, we consider the engineering of states with nonzero quasimomentum k , with $k = \pm k_1$. If the spin chain is in this particular state, then the expectation value $[\langle \cos(k_1) - \cos(k) \rangle]^2$ is zero. Hence to generate $|\pm k_1\rangle$ states, we may use the expectation value $[\langle \cos(k_1) - \cos(k) \rangle]^2$ as a minimizing function (instead

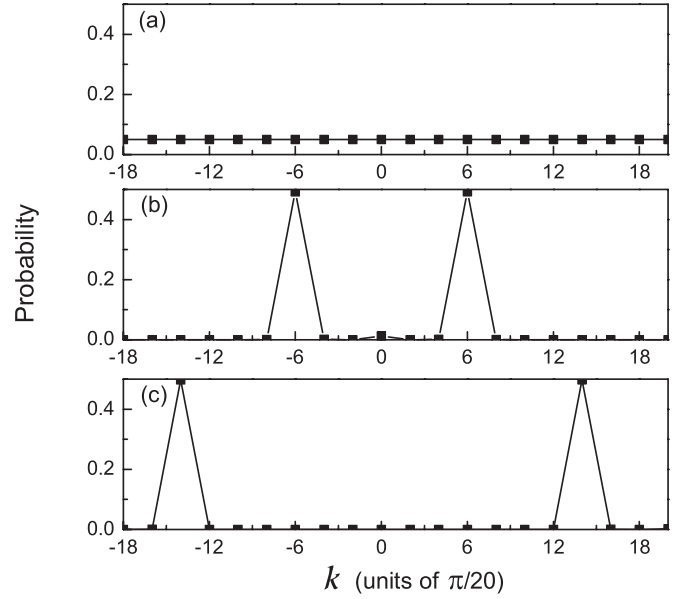


FIG. 6. Probability distribution in the quasimomentum state space of a Heisenberg chain of 20 spins. Panel (a) is the initial distribution, panels (b) and (c) represent the distribution obtained after applying 80 pulses with $[\langle \cos(6\pi/N) - \cos(k) \rangle]^2$ and $[\langle \cos(14\pi/N) - \cos(k) \rangle]^2$ as the minimization functions. Here the strength of the pulses C is varied in the range of $[0.001, 10]$ and the free evolution time t of the chain between two neighboring kicks is varied in the range of $[0.001, 100]$.

of D defined above) in our control scheme. We examined this possibility using a chain of 20 spins, with a spin excitation located at the center of the chain at time zero. The momentum distribution profile of this initial state is shown in Fig. 6(a). To generate a state with quasimomentum $k = \pm 6\pi/20$ as an example, we apply a total of 80 kicks of strength C_j in the interval $[0.001, 10]$. Also, the free evolution time t_j between the two neighboring kicks is optimized in the range $[0.001, 100]$. The minimization function is chosen to be $[\langle \cos(6\pi/20) - \cos(k) \rangle]^2$. Results obtained under this control scheme are shown in Fig. 6(b). It is seen that both quasimomentum states with $k = \pm 6\pi/20$ are equally populated. More than 49% probability in each of the two target states indicates that our scheme is again highly efficient. Another numerical example is shown in Fig. 6(c) where the results are obtained by using the minimization function $[\langle \cos(14\pi/20) - \cos(k) \rangle]^2$ for optimizing 80 kicks. About 49% population in both states of $k = \pm 14\pi/20$ is observed. Note also that the final produced states here are nonstationary states and hence they will evolve in time after turning off the parabolic field. However, the population distribution of these states in the quasimomentum space remains almost the same.

Encouraged by the success of our scheme in engineering quasimomentum states other than the $|k = 0\rangle$ state, we further test our scheme for generating the superposition of quasimomentum states. As a computational example, we let the state to be engineered be an equal superposition state $[|k_1\rangle + |-k_1\rangle + e^{i\phi}(|k_2\rangle + |-k_2\rangle)]/2$. We found from our numerical experiments that this can also be done by using a more complicated minimization function.

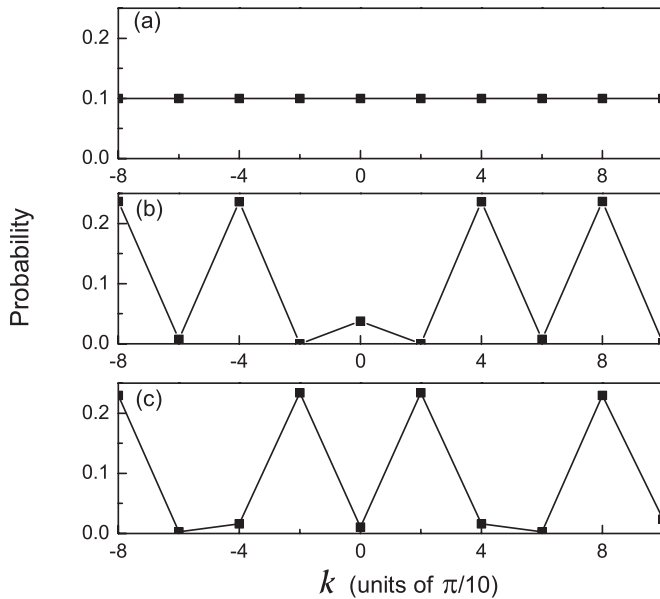


FIG. 7. Probability distribution of the quasimomentum states of a Heisenberg chain of 10 spins. Panel (a) corresponds to the initial state. Panels (b) and (c) correspond to the resulting state obtained after applying 80 pulses with $(2|c_{k_1}^n|^2 - 0.5)^2 + (2|c_{k_2}^n|^2 - 0.5)^2 + 2(\theta - \phi)^2$ as the minimization function. For panel (b), $k_1 = 4\pi/10$, $k_2 = 8\pi/10$, and $\phi = 0$. For panel (c), $k_1 = 2\pi/10$, $k_2 = 8\pi/10$, and $\phi = \pi/2$. The field strength parameter C is varied in the interval of $[0.001, 10]$, whereas the free evolution time t between two neighboring kicks is varied in the interval of $[0.001, 100]$.

Specifically, we optimize the parameters C_j and t_j for each kick by minimizing the function $(2|c_{k_1}^n|^2 - 0.5)^2 + (2|c_{k_2}^n|^2 - 0.5)^2 + 2(\theta - \phi)^2$, where $c_{k_1}^n$ and $c_{k_2}^n$ are the probability amplitudes on the quasimomentum states $|k_1\rangle$ and $|k_2\rangle$ right after the n th kick and θ is the phase difference between the k_1 and k_2 components. So if the target state is reached, then the value of the above minimization function becomes zero. The results of our calculations with the initial state $|\mathbf{5}\rangle$ for a chain of 10 spins are shown in Fig. 7. In Fig. 7(b) an engineered equal superposition state $[|k = 4\pi/10\rangle + |k = -4\pi/10\rangle + |k = 8\pi/10\rangle + |k = -8\pi/10\rangle]/2$ is shown. The field strength parameters C_j are limited to the interval $[0.001, 10]$. The free time evolution parameters t_j are varied in the interval $[0.001, 100]$. Initially, the minimization function

has a value of 0.09. After applying 80 optimized kicks, the value of the minimization function reduces to 0.00534, with $|c_{\pm k_1}^{80}|^2 = 0.2364$ and $|c_{\pm k_2}^{80}|^2 = 0.2367$, quite close to the probability distribution required for the desired state. Further, our numerical calculation shows that the phase difference θ in the end is -2.3352×10^{-4} , which is close to the ideal value of the target state with $\phi = 0$. Another example is displayed in the bottom panel of Fig. 7, where a state $[|k = 2\pi/10\rangle + |k = -2\pi/10\rangle + e^{i\pi/2}(|k = 8\pi/10\rangle + |k = -8\pi/10\rangle)]/2$ (an equal superposition of four quasimomentum states with a $\pi/2$ phase difference between two pair of quasimomentum states) is targeted. Before applying the kick to the initial state $|\mathbf{5}\rangle$, the minimization function has a value 2.557. Using our control scheme, the value of the minimization function reduces to 0.00626 after 80 optimized kicks, with $|c_{\pm k_1}^{80}|^2 = 0.2341$ and $|c_{\pm k_2}^{80}|^2 = 0.2297$, and the phase difference between k_1 and k_2 components found to be 1.5708 (a value very close to the target value $\pi/2$). It is hence evident now that our scheme can be generalized to engineer arbitrary superposition of quasimomentum states of a Heisenberg spin chain.

IV. CONCLUSION

A robust and scalable scheme for multipartite W state generation can bring us one step closer to realizing a test bed in understanding many-body entanglement. In this work, we have proposed a simple scheme for the generation of W states in a Heisenberg spin chain by exploiting the mapping between a kicked spin chain and a quantum kicked rotor. Based on this mapping, we are able to use the idea of accumulative angular squeezing from the quantum rotor context for the engineering of W states or other more general target states. We have numerically studied our scheme and showed that W states can be generated with high fidelity. The most noteworthy feature of our scheme is that it applies to long spin chains without modifications (thus indicating its scalability), with the large N -limit equivalent to the known problem of angular squeezing of a kicked rotor. Since our theoretical considerations have exploited the single excitation subspace afforded by the conservation of the total polarization of the spin chain, in experimental implementations efforts should be made to suppress possible transitions to other subspaces.

-
- [1] M. A. Nielsen and I. L. Chuang, *Quantum Computation and Quantum Information* (Cambridge University Press, Cambridge, England, 2000).
 - [2] R. Horodecki, P. Horodecki, M. Horodecki, and K. Horodecki, *Rev. Mod. Phys.* **81**, 865 (2009).
 - [3] C. H. Bennett, G. Brassard, C. Crépeau, R. Jozsa, A. Peres, and W. K. Wootters, *Phys. Rev. Lett.* **70**, 1895 (1993).
 - [4] N. Gisin, G. Ribordy, W. Tittel, and H. Zbinden, *Rev. Mod. Phys.* **74**, 145 (2002).
 - [5] A. M. Childs and W. van Dam, *Rev. Mod. Phys.* **82**, 1 (2010).
 - [6] W. Dur, G. Vidal, and J. I. Cirac, *Phys. Rev. A* **62**, 062314 (2000).
 - [7] H. J. Briegel and R. Raussendorf, *Phys. Rev. Lett.* **86**, 000910 (2001).
 - [8] H. Haffner *et al.*, *Nature (London)* **438**, 643 (2005).
 - [9] D. Bruß, D. P. DiVincenzo, A. Ekert, C. A. Fuchs, C. Macchiavello, and J. A. Smolin, *Phys. Rev. A* **57**, 2368 (1998); J. Joo, Y.-J. Park, S. Oh, and J. Kim, *New J. Phys.* **5**, 136 (2003).
 - [10] T. Yamamoto, K. Tamaki, M. Koashi, and N. Imoto, *Phys. Rev. A* **66**, 064301 (2002); M. Eibl, N. Kiesel, M. Bourennane, C. Kurtsiefer, and H. Weinfurter, *Phys. Rev. Lett.*

- 92**, 077901 (2004); H. Mikami, Y. Li, K. Fukuoka, and T. Kobayashi, *ibid.* **95**, 150404 (2005); P. Walther, K. J. Resch, and A. Zeilinger, *ibid.* **94**, 240501 (2005); T. Tashima, S. K. Özdemir, T. Yamamoto, M. Koashi, and N. Imoto, *Phys. Rev. A* **77**, 030302(R) (2008); *New J. Phys.* **11**, 023024 (2009); S. B. Papp, K. S. Choi, H. Deng, P. Lougovski, S. J. van Enk, and H. J. Kimble, *Science* **324**, 764 (2009); R. Ikuta, T. Tashima, T. Yamamoto, M. Koashi, and N. Imoto, *Phys. Rev. A* **83**, 012314 (2011).
- [11] C. S. Yu, X. X. Yi, H. S. Song, and D. Mei, *Phys. Rev. A* **75**, 044301 (2007); I. E. Linington and N. V. Vitanov, *ibid.* **77**, 010302(R) (2008); J. Song, Y. Xia, and H.-S. Song, *ibid.* **78**, 024302 (2008); H.-F. Wang, X.-Q. Shao, Y.-F. Zhao, S. Zhang, and K.-H. Yeon, *J. Phys. B* **42**, 175506 (2009); D. Gonta and S. Fritzsche, *Phys. Rev. A* **81**, 022326 (2010).
- [12] K. Fujii, H. Maeda, and K. Yamamoto, *Phys. Rev. A* **83**, 050303(R) (2011).
- [13] X. Wang, *Phys. Rev. A* **64**, 012313 (2001).
- [14] I. D’Amico, B. W. Lovett, and T. P. Spiller, *Phys. Status Solidi C* **5**, 2481 (2008).
- [15] L. F. Santos, *Int. J. Quantum Inform.* **4**, 563 (2006).
- [16] T. Boness, S. Bose, and T. S. Monteiro, *Phys. Rev. Lett.* **96**, 187201 (2006).
- [17] I. Sh. Averbukh and R. Arvieu, *Phys. Rev. Lett.* **87**, 163601 (2001).
- [18] J. B. Gong and P. Brumer, *Phys. Rev. A* **75**, 032331 (2007); V. Balachandran and J. B. Gong, *ibid.* **77**, 012303 (2008); **79**, 012317 (2009).
- [19] W. H. Oskay, D. A. Steck, and M. G. Raizen, *Phys. Rev. Lett.* **89**, 283001 (2002).
- [20] M. Leibscher and I. Sh. Averbukh, *Phys. Rev. A* **65**, 053816 (2002).
- [21] W. H. Press, B. P. Flannery, S. A. Teukolsky, and W. T. Vetterling, *Numerical Recipes in Fortran 77: The Art of Scientific Computing* (Cambridge University Press, Cambridge, England, 1992).
- [22] D. A. Meyer and N. R. Wallach, *J. Math. Phys.* **43**, 4273 (2002).